Desalination and Water Treatment
www.deswater.com

doi:10.5004/dwt.2017.20825

79 (2017) 386–399
June

Biosorption of Indigo and Acid Yellow 2G (Y2G) dyes from aqueous solutions using a commercial powder form of ecologically pure *Hawaiian Spirulina pacifica* (HSP)

Arda Yalcuk*, Gamze Dogdu Okcu

Department of Environmental Engineering, Faculty of Engineering and Architecture, Abant Izzet Baysal University, Golkoy Campus-Bolu, Turkey, email: ayalcuk@gmail.com (A. Yalcuk), dogdu.gamze@gmail.com (G.D. Okcu)

Received 12 December 2016; Accepted 13 April 2017

ABSTRACT

This study focuses on the removal of commercial Acid Yellow 2G and Indigo dyes by using biosorbent *Hawaiian Spirulina pacifica (HSP).* It studies the effects of pH, the initial dye concentration, the biosorbent dose and the agitation speed and temperature, on the removal of dyes. Thermodynamic parameters indicated the exothermic and spontaneous characteristics of biosorption. Langmuir, Freundlich and Temkin adsorption isotherms were applied to examine the efficiency of *HSP.* Fourier transform infrared spectroscopy (FTIR) and scanning electron microscopy (SEM) images proved moderate adsorption of dyes onto *HSP.* The results shows that this commercial, ecological, low-cost and natural nutrient biosorbent may be useful for the removal of toxic and hazardous textile dyes from aqueous solutions.

Keywords: Biosorption; *Hawaiian Spirulina pacifica (HSP)*; Indigo; Acid Yellow 2G (Y2G)

1. Introduction

Dyes are colored organic matter that are released in effluent waters by many industrial facilities dealing with textiles, dye manufacturing, leather, paper, paint, rubber, plastic, pesticides, wood preserving chemicals, printing, food and cosmetics [1–3]. While approximately 60% of them alone are consumed by the textile sector to color different kinds of fabrics, 1–15% of the dyes are lost in the effluents during the dyeing process [2,4–7]. Dyes generally have a synthetic origin and complex aromatic structures that mean they are non-degradable and are hard to breakdown. If the dye-containing wastewater discharged from the industries mentioned earlier is not properly treated, it can pose aesthetic problems; it can affect light penetration in aquatic systems and thereby reduce gas solubility and photosynthesis within aqueous flora [8–10]. Besides their biologically non-degradable properties, they are toxic to some aquatic organisms and cause serious health risks to humans [11]. Dyes have many structural types and are classified both by their chemical structure and their application to types of fiber [12]. In addition, dyes are also classified on the basis of their solubility; soluble dyes can be acid mordant, metal complex, direct, basic and reactive; insoluble dyes include vat, disperse, sulfur and azoic types [4]. The treatment of water-soluble, reactive and acid dyes is of considerable significance, because conventional systems are ineffective in treating them [13]. Sixty to seventy percent of dyes used in the textile industry are azo dyes; molecules with one or more azo (N=N) bridges linking substituted aromatic structures [14]. Industrial synthetic complex azo dyes are produced to be resistant to washing, chemical solvents, sunlight and microbial attacks [15]. Azo dyes are highly water soluble due to the presence of SO_3^-, COO^-, and OH^- groups, and their degradation products are highly carcinogenic [16]. Nitrogen–nitrogen double bonds and sulfonate groups in the structure make these dyes stubborn to treat [17]. Acid Yellow 2G (Y2G), a monoazo dye, is commonly used in dye-

*Corresponding author.

ing wool, silk, cotton, leather, paper and hot stamping foil. In addition, it is a general additive of ordinary household products such as shampoos, bubble baths, shower gels, liquid soaps, multipurpose cleansers, dishwashing liquid and alcohol-based perfumes [18,19]. Yellow 2G is easily dissolved in water and causes serious health hazards like allergies, asthma and hyperactivity, so its usage is restricted and it could be banned in the near future [20].

Vat dyes are used for cotton – mainly consisting of cellulose fibers – as soluble leuco salts, and for rayon and wool as well. These kinds of dyes are water-insoluble dyes whose chemical class contains anthraquinone (including polycyclic quinones) and indigoids [4]. Indigo ($C_{16}H_{10}N_2O_2$), one of the oldest known blue dyes, is still employed extensively today for dyeing cotton yarn in the manufacture of denim and blue jeans. The current annual consumption of Indigo and other vat dyes is about 33 million kg [21,22]. About 15% of the Indigo used is lost during the dyeing process [23]. Indigo is moderately persistent and its bioaccumulation potential is low. The acute toxicity of this dye is low via oral, inhalation and dermal routes. Although Indigo shows lower acute and chronic toxicity, it is quietly stubborn and its degradation is low [24]. Due to local legal obligations, the effluents of the textile industry or textile dyes have to be treated carefully before discharge. For this purpose, some conventional methods such as adsorption, sedimentation, chemical analysis, chemical coagulation, biological methods and advanced oxidation procedures have been used to meet regulatory discharge standards [11,25,26]. Yet, when all treatment methods are looked at in detail, they are not feasible for treating dye-rich wastewater because they are technology intensive, have a demand for reliable power, feature complex components, unproven long-term effectiveness, and have high investment and maintenance costs [27]. Among these methods, adsorption is regarded to be superior due to several advantages such as simple design, ease of operation, low-cost and insensitivity to toxic materials [28]. Recently, biosorption (adsorption on biomass) has been widely used due to its suitability for water treatment [29]. Biosorption can be defined as the passive uptake of organic or inorganic species from aqueous solutions by microbial biomasses (bacteria, yeasts, filamentous fungi and algae) [30]. This process is the combination of physical and chemical adsorption, electrostatic interaction, ion exchange, complexation, chelation and micro-precipitation that take place at the cell-wall level [31]. Dead cells are not affected by chemicals and toxic wastes, and they do not pollute the environment by releasing toxins. So, they are generally preferable for dye removal studies [1].

Table 1 shows recent studies that include Y2G, Indigo or *Spirulina platensis*. There are limited studies on the removal of textile dyes using *Spirulina platensis* or its sub-strains.

To our knowledge, no studies in published literature have been reported until now on the biosorption capacity of *S. pacifica* for any dyes. *HSP* is a kind of blue-green micro algae that is also a strain of *S. platensis.* Furthermore, it is one of the few studies that have been carried out on the treatment of Indigo and Yellow 2G textile dyes [1,18,32–34].

In this study, *Hawaiian Spirulina pacifica (HSP)* was used for the biosorption of Indigo and Yellow 2G in a batch system. The first goal was to analyze the effects of pH, temperature, initial dye concentration and the amount of biosorbent on the biosorption capacity of *S. pacifica*. In order to investigate the impacts of temperature in detail, a thermodynamic analysis was performed measuring the Gibbs free energy ($\Delta G°$), the enthalpy ($\Delta H°$) and the entropy ($\Delta S°$). Langmuir, Freundlich and Temkin isotherm models were applied to the experimental data and isotherm constants were calculated. Furthermore, FTIR, SEM, energy dispersive spectroscopy (EDS) analyses were conducted to investigate the interaction of the dye with the biomass involved in the Indigo and Y2G biosorption process.

Table 1
List of studies for *Spirulina platensis* and various adsorbents for Y2G and Indigo dyes

DYE	Adsorbent/Biosorbent	Referances
Yellow 2G	İnactive aerobik granule	[18]
Yellow 2G	Nanoparticle biospolymer	[32]
Yellow 2G	Nonliving aerobic granule	[33]
Yellow 2G	Chlora vulgaris	[34]
Yellow 2G	Active carbon ranbutam	[35]
Yellow 2G	Orange peel	[36]
Yellow 2G	Calcinate alunite	[37]
Indigo	Aspergilus alliaceus	[1]
Indigo	Active carbon	[38]
Indigo Carmine	Activeted sewage sludge	[39]
Indigo Carmine	Pyrolysed sewage sludge	[39]
Acid Blue and FD&C Red no 40	Sipirulina planthesis	[40]
CI Basic Red 46	Sipirulina planthesis	[41]
Reactive red 120	Spirulina planthesis	[8]

2. Experimental analysis

2.1. Biosorbent

Spirulina is a kind of blue-green micro algae that cannot be seen by the naked eye. It is usually grown in warm and brackish water. Spirulina contains between 60 to 70% complete, digestible proteins that contains 18–22 amino acids – including 8 essential amino acids. *Spirulina* biomass is a rich source of vitamins A, B and E, of thousands of enzymes, of dozens of minerals, trace elements and chlorophyll [42]. *Spirulina Pacifica*® biomass is carefully grown in ponds in Hawaii – using sea water from a depth of 2000 feet to process the algae – and is used to create the world's finest pure available *Spirulina* biomass powder and *Spirulina* biomass tablets (Cyanotech Corp./ Hawaii-ABD) [43]. *HSP* is sub-strain of *Spirulina platensis,* and it has extremely high phycocyanin pigment content (Fig. 1). Dead *S. pacifica* biomass is produced by anaerobic chill-drying and chill-tableting techniques called "Ocean Chill Drying", which don't use any chemicals or heat treatment, and preserves the organic or inorganic content

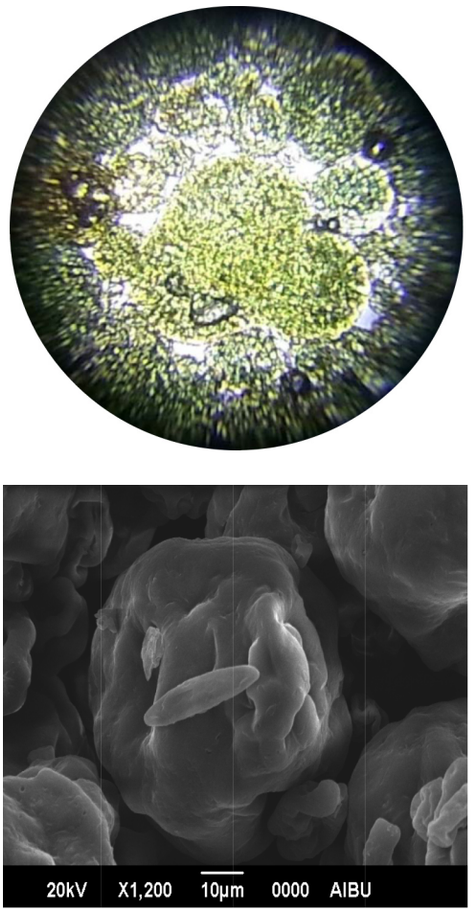

Fig. 1. General appearance of the *Spirulina pacifica* (a) Light micrograph, SOIF (b) SEM image.

in powder or tablet form [42]. The general properties and composition of the biosorbent that was used in our study is given in (see Supplementary material).

2.2. Dyes

Commercial Acid Yellow 2G dye (Acid Yellow 17, molecular formula: $C_{16}H_{10}Cl_2N_4Na_2O_7S_2$) and 40% commercial synthetic blue Indigo dye dissolved in water (Molecular formula: $C_{16}H_{10}N_2O_2$) were supplied by the Realkom Denim Textile Factory in Düzce/Turkey and were used without any purification to simulate realistic economic and operating conditions. Fig. 2 illustrates the chemical structure of the Yellow 2G and Indigo dyes. All the solutions used in the experiment were obtained by diluting the 1000 mg/L stock Y2G and Indigo blue solutions, which were prepared by dissolving accurately weighted dye in distilled water at different concentrations. The concentrations of dye solutions were determined by a UV/Vis (Merck Pharo 100 model) spectrophotometer at the maximum absorbance wavelength values (λ_{max}) of 61 nm for commercial Indigo dye and 390 nm for the commercial Acid Yellow 2G dyes.

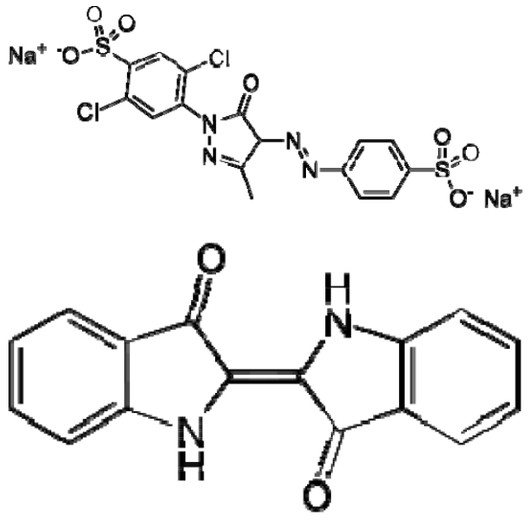

Fig. 2. Chemical structures of (a) Acid Yellow 2G (Acid Yellow 17) (b) Indigo.

2.3. Batch biosorption studies

The removal of commercial textile dyes by *HSP* was studied using a batch technique. Samples with different dye concentrations were prepared by diluting 1000 mg/L of stock dye solution with de-ionized water. The study used 200 mL samples of *HSP* biosorbent. Solutions of 0.1 M NaOH and 0.1 M H_2SO_4 were used for pH adjustments. The temperature was controlled using an isothermal shaker. The biosorbent dosage was varied from 1.0 to 6.0 g. The two common techniques to separate the adsorbent from the aqueous solution and analyze the liquid portion for the final, residual, sorbate concentration at equilibrium are filtration [44] and centrifugation [45]. Filtration was not chosen in these experiments because some dyes can be absorbed into the filter paper. The flasks were agitated on a shaker at 100 rpm for a pre-determined time at a constant temperature of 25 ± 1°C. After equilibrium was reached, 10 mL of the suspension was centrifuged in a stoppered tube for 15 min at 4100 rpm; 5 mL of the dye solution was taken from the tube, measured using a filtered syringe to guarantee the accuracy, and instantly chemically analyzed [33]. The impacts of pH, contact time, initial dye concentration, biosorbent dose, agitation speed and temperature were investigated individually to determine the ideal experimental conditions for both the commercial Indigo and Acid Yellow 2G dyes. Using optimum conditions, the dye removal capacity, kinetic studies, thermodynamic experiments and equilibrium values were determined in a temperature range from 20 to 45°C, and the initial dye concentrations ranged from 50 to 300 mg/L.

2.4. Analyses

The removal of commercial textile dyes by the biosorbent was studied using a NUVE ST-30 model shaker. A Thermo Scientific Orion 5 Star series pH meter was used for pH adjustments. Before analysis, the pH of all the samples was readjusted to an initial pH value. A NUVE

NF-400 model centrifuge was used to separate the solid phase from the liquid phase. FTIR spectral analysis was recorded on a Shimadzu IRPrestige-21 infrared spectrometer in the region from 400 to 4000 cm^{-1} to determine the functional groups in the interaction between biosorbent and dyes. In the study, SEM analyses were also performed using a JEOL JSM-6390LV type SEM. To calculate dye concentrations from the absorbance values of solutions, the calibration curve used was one that was easily reproducible and linear over the concentration range. Absorbance values were recorded at the corresponding maximum absorbance wavelength (λ_{max}), and the dye solutions were initially calibrated for concentrations in terms of absorbance units [1].

The adsorbed amounts and the biosorption capacity were calculated using the following equation:

$$\text{Removal percentage (R)} = \frac{(C_0 - C_t)}{C_0} \times 100 \quad (1)$$

C_0 and C_t (mg/L) are the initial and final concentration of the dye solutions. The biosorption capacity of the *HSP* biosorbent was calculated using the following equation:

$$q = \frac{(C_0 - C_e)V}{W} \quad (2)$$

where q (mg/g) is the amount of dye adsorbed by the biosorbent, C_0 and C_e (mg/L) are the initial and equilibrium liquid phase concentrations of the dye solutions; V (L) is the initial volume of the dye solution and W (g) is the weight of the biosorbent.

3. Results and discussion

3.1. FTIR analysis of the biosorbent

FTIR spectra for the *HSP* biosorbent powder were taken over a range from 400 to 4000 cm^{-1} to obtain information on the nature of functional groups and interactions of the dyes and biosorbent at the surface of the biosorbent. Fig. 3 shows the changes in the FTIR spectra of *S. pacifica* before and after dye biosorption. The FTIR spectrum of unloaded *S. pacifica* biomass is shown in Fig. 3 indicating several major bands: around 3286.70 cm^{-1}, 1647.21 cm^{-1}, 1450.17 cm^{-1} and 1149.57 cm^{-1} [46]. The spectra presented in Fig. 3 show important similarities identified by the reports in previous studies [18]. The strong bands at 3280.92 and 3278.99 cm^{-1} could reflect the overlapping of N–H and O–H stretching vibrations of hydroxyl and amine groups on the surface of *S. pacifica* [47,48], and the band at 2968.80 cm^{-1} exhibits an asymmetric vibration of CH_2 [8,9,49]. A distinct band at 1647.21 cm^{-1} represented the stretching vibration of C–O and C–N (amide I) peptide bonds in protein [9,46,50], while the 1535.34 cm^{-1} band might be due to the stretching vibration of C–N and the deforming vibration of N–H (Amide II) peptides in protein [8,18]. The band at 1074.35 cm^{-1}might be attributed to the stretching vibration of the –OH of polysaccharides. The adsorption bands in the region from 750 to 900 cm^{-1} can be attributed to P–O, S–O and aromatic C–H stretching vibrations [8]. The 3286.70 cm^{-1}, 2968.80 cm^{-1} and 1647.21 cm^{-1} band intensities all decreased, suggesting that

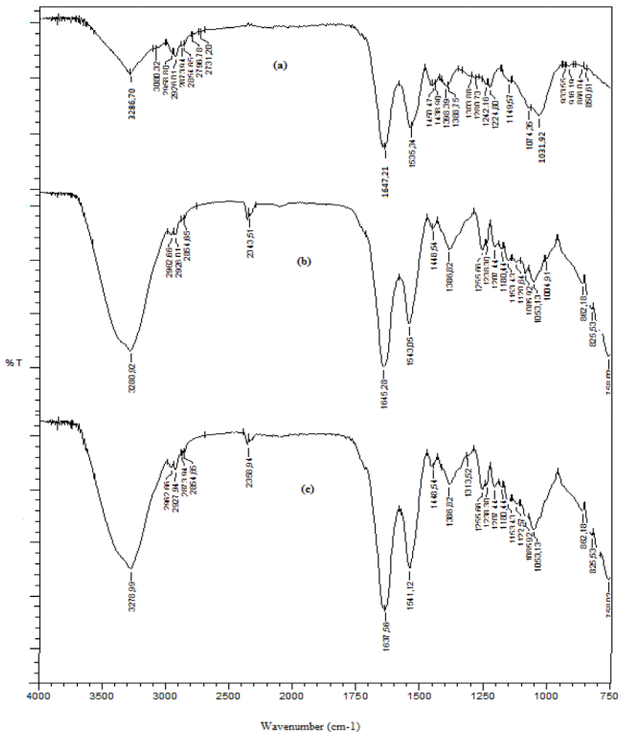

Fig. 3. FTIR spectra of the unloaded (a) Y2G dye-loaded (b) Indigo dye-loaded biomass (c).

N–H and O–H of hydroxyl and amine, the CH_2 groups of lipids and the C=O all carboxylate after *S. pacifica* biosorption, especially after Indigo dye biosorption (Table 2).

The bands at 1280.73 cm^{-1} and 1031.92 cm^{-1} can be assigned to C–N stretching of amide and amine groups that were shifted to 1238.80 cm^{-1} and 1053.13 cm^{-1} and may probably be involved in the biosorption process [8,48,51]. The aldehydes and ketones groups could be observed at 1398.39 cm^{-1} and 1149.57 cm^{-1}, respectively [48]. The peak at 1450.17 cm^{-1} represents –N–H bending vibrations (especially bending of NH_4^+) for *S. pacifica* [52]. According to the results obtained in published literature, the interaction between dyes and *S. pacifica* biosorbent should occur with the OH, NH_2, C=O, COO groups and the aromatic groups present in the biomass [8,9,48,49,53]. Therefore, the FTIR results show that the main chemical functional groups involved in biosorption of Y2G and Indigo onto *S. pacifica* biomass are amine, hydroxyl, carboxyl or a combination of carboxyl, amine and hydroxyl groups.

3.2. SEM analysis

Investigation of the surface area and structural morphologies of the materials are obtained by SEM analysis. In the study, SEM images of the biosorbent used were taken before and after the adsorption process in order to examine the suitability of the *HSP* biosorbent. Fig. 4–c present the SEM images of the biosorbent before and after commercial Acid Yellow 2G and Indigo dye biosorption, respectively.

Table 2
The FTIR characteristics absorbance peaks of unloaded, Y2G and Indigo dye loaded HSP

Before	Y2G After	Indigo After	Functional group assigned
3286.70	3280.92	3278.99	O–H and N–H stretching
2968.80	2962.66	2962.66	CH stretching
–	2343.51	2358.94	C≡N stretching
1647.21	1645.28	1637.56	C=O stretching (Amide I) N–H
1535.34	1543.05	1541.12	C–N stretching (Amide II)
1450.17	1448.54	1448.54	N–H bending with CH_2 deformation
1398.39	1386.82	1386.82	C–O–H bending
1280.73	1238.80	1238.80	NH bending (Amide III)
1149.57	1153.43	1153.49	C–O stretching
1074.35	1085.92	1085.92	P–O, S–O and C–H stretching
1031.92	1053.13	1053.13	
933.66	–	–	
916.18	–	–	P–O, S–O and aromatic sytetching vibrations
866.04	862.18	862.18	
850.61	825.53	825.33	

Conditions for Y2G is; pH 2, 5 g/L biomass, 150 mg/L, 150 rpm, 25°C, 120 min; for Indigo dye is; pH 2, 3 g/L biomass, 100 mg/L, 100 rpm, 25°C, 120 min

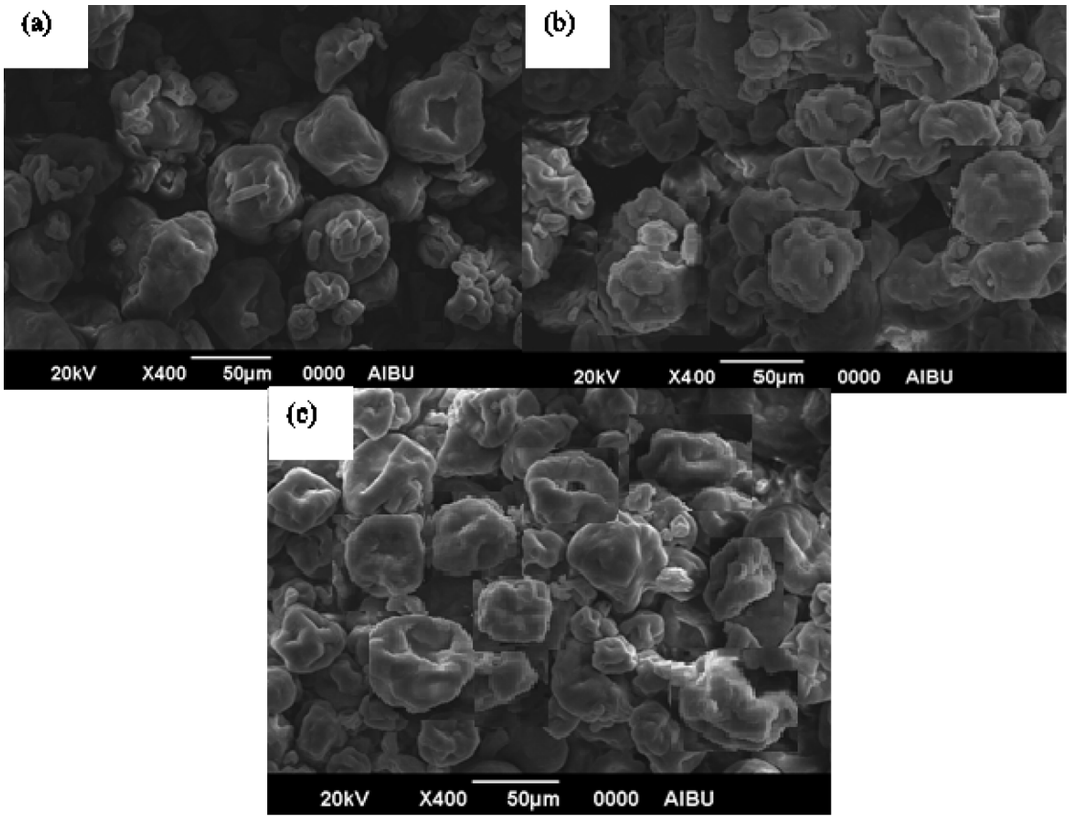

Fig. 4. SEM images of sample (a) *Spirulina pacifica*; (b) Acid Yellow 2G dye biosorbed by *Spirulina pacifica* (c) Indigo dye biosorbed by *Spirulina pacifica*.

As seen from Fig. 4a, the SEM images of the biosorbent samples show considerable numbers of rough holes and irregularities on the surface of the biosorbent that offer a good possibility to trap the dye molecules and allow biosorption into these holes. The porous surface has been covered by dye molecules and particle density has increased after the biosorption process, Fig. 4b and 4c.

3.3. Effect of experimental conditions on biosorption capacity

3.3.1. Effect of pH

The initial pH of the dye solution strongly affects the surface charge of the biosorbents, as well as the degree of ionization of different pollutants or functional groups of the adsorbate, resulting from the changing amount of adsorbed dye [11,54]. Generally, the initial pH of the dye solutions improves or suppresses dye uptake, surface characteristics and the chemical specialties of the dyes [55,56]. The hydrogen and hydroxyl ions are adsorbed, and adsorption of other ions is affected by the pH of the solution. The biosorption process is affected by a change of pH through dissociation of functional groups on the active sites of the biosorbent surface, which leads to a shift in the reaction equilibrium characteristics of the biosorption process [47]. In this study, the biosorption of Y2G and Indigo onto *S. pacifica* was studied for different pH values (2.0, 3.0, 4.0, 6.0, 8.0, and 10.0). In the experimental work, 1.0 g of *S. pacifica* biosorbent was added to 200 mL of a 100 mg/L dye solution. Samples were shaken for 120 min at an agitation speed of 100 rpm at 25 ± 1°C. Fig. 5 shows that dye removal was lower at alkaline pH values. As the pH increased from 1.0 to 2.0, the biosorption capacity reached a maximum value of 81.53% (16.30 mg/g) for Y2G and 86.08% (17.22 mg/g) for Indigo dyes. However, the biosorption equilibrium capacity decreased as the pH increased from 2 to 3. When the pH increased further (> 4.0), the biosorption process was decreased and even restricted, resulting in a biosorption capacity of 6.88% (1.32 mg/g) for Y2G and approximately 0% (0.1 mg/g) for Indigo dyes. Similar results were reported in other studies [1,11,18,32,57–59]. Cardoso et al. [8] stated in their articles that under acidic conditions (pH 2.0 to 3.0), the *S. platensis* surface was positively charged as a result of the protonation of the OH, NH_2, C=O and COO groups. Dotto et al. [48] stated in their article that the point of zero charge of *S. platensis* algae is at a pH value of 7. Moreover, *HSP* is a sub-strain of the *Spirulina platensis* that was mentioned in Section 2.1 and similar zero point of charge effects were seen for the biosorption trend varying by pH value (Fig. 5).

Likewise with *S. platensis*, as shown in Fig. 3 (FTIR), weak base groups on the biosorbent surface like OH^-, NH_2 and C=O could protonate and have a positive charge when the solution pH is lowered. Therefore, under acidic conditions, a significantly high electrostatic attraction can exist between the positively charged surface of the biosorbent (*Spirulina pacifica*) by absorbing H^+ ions and the dye molecules. This effect was largely related to the anionic characters of Y2G and Indigo dyes. Similar results were reported for the pH effect on the biosorption of Acid Yellow 17 on aerobic granular sludge [33]. As an anionic dye, Y2G will dissociate into the anionic forms (D–SO_3) in aqueous

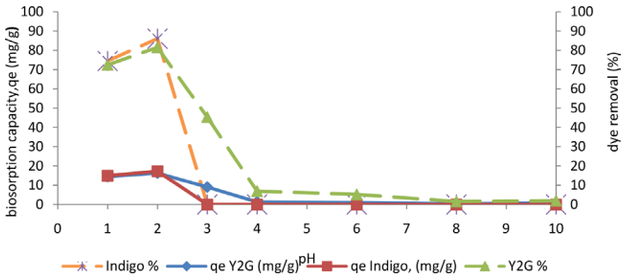

Fig. 5. The effect of initial pH on the equilibrium biosorption of *S. pacifica*. Experimental conditions: C_o: 100 mg/l, biomass: 1 g/l, temperature: 25°C, agitation rate: 100 rpm, and time 120 min.

solution [33,48]. In this way, there would be electrostatic interactions between the dyes sulfonated groups and the biosorbent surface [48]. Likewise with the *S. platensis* biosorption mechanism, when the pH of the solution is lower than 7 (pH_{zpc}), Y2G and Indigo uptake will be increased by the electrostatic force of attraction. When the pH of the system increases beyond 7, the negatively charged surface sites do not encourage biosorption, because higher OH^- generation causes competition between OH^- and dye anions, and finally, the dye biosorption decreases [60]. All the following experimental studies have been performed by adjusting the pH value to 2.

3.3.2. Effect of biosorbent dose

The effect of the biosorbent dose was investigated in order to evaluate the maximum biosorption capacity. Biosorption efficiencies can be improved by increasing the biosorbent dosage, which can be explained by the increase of surface area where the adsorption can take place [3]. The biosorbent dosage was varied over 1, 2, 3, 4, 5 and 6 g/L at a fixed pH, temperature and dye concentration. It can be seen that the dye removal rapidly increased with an increased biosorbent dose from 1 to 2 g/L for both dyes, and after 2 g/L, dye removal was slightly increased as shown in Fig. 6.

This could be due to the fact that active sites were effectively utilized when the dosage was still low. For Y2G, the maximum biosorption was obtained at 82.82% for a 5 g/L (1g) *HSP* dosage. The optimum *S. pacifica* concentration was determined to be 5 g/L (1 g) as the biosorption process reached equilibrium at this dosage and slightly decreased with increasing dosage amounts. Gao et al. [33] studied Acid Yellow 17 (Y2G) adsorption on non-living aerobic granular sludge in their articles, and they reported that maximum removal efficiency was 86% at an adsorbent concentration of 3 g/L. Moreover, Rakhshaee [32] indicated that the percentage removal of Acid Yellow 17 increased with increasing dosage of Fe° nanoparticles (NP) of 0.5 to 30.0 g/L was used from 23.1% to 61.5%. It could be due to increasing the reactive sites with Fe^0 NPs which remove the dye molecules through reduction.

For Indigo dye, Fig. 6 shows that the increase in biosorbent dosage from 1 to 3 g/L resulted in an increase in the dye removal percentage from 56.86% to 84.53%. The increase in the removal rate of Indigo can be explained by

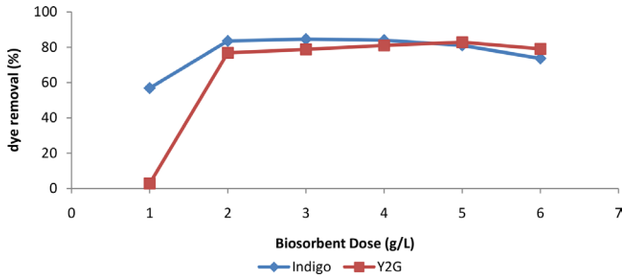

Fig. 6. The effect of biosorbent dosage on the equilibrium biosorption of *S. pacifica*. Experimental conditions: C_o: 100 mg/l, pH 2, temperature: 25°C, agitation rate: 100 rpm, and time 120 min.

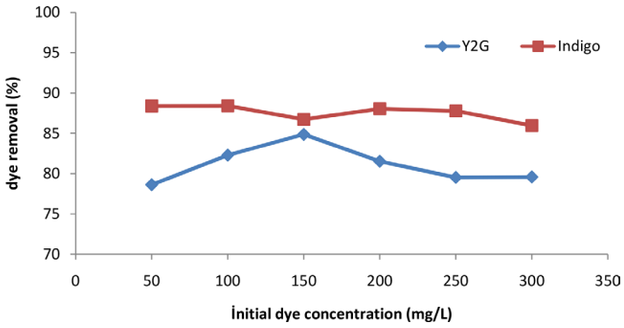

Fig. 7. The effect of initial dye concentration on the equilibrium biosorption of *S. pacifica*. Experimental conditions: biomass:5 g/L, temperature: 25°C, pH 2, 100 rpm and time 120 min for Y2G; biomass: 3 g/L, temperature: 25°C, pH2, 100 rpm and time 120 min for Indigo.

the increased surface area of the biosorbent and that dye molecules could find more available binding sites [57]. After 3 g/L, the biosorption efficiency didn't significantly change with increasing dosages of *S. pacifica* from 3.0 to 6.0 g/L. The reason for this is the binding of almost all Indigo dye ions onto the biosorbent surface and better contact being established between the biosorbent particles and the Indigo dye molecules – with a smaller amount of biosorbent in the solution [57,61]. From another perspective, when the amount of *HSP* began to increase beyond 3 g/L, the *HSP* particles would contribute to the aggregation of biosorbent particles and lead to a reduction in the total surface area of the biosorbent. This would result in an increment in the diffusion path length [62].

3.3.3. Effect of initial dye concentration

The dye concentration has an important effect on the biosorption process [62]. When all molecules are transferred between the aqueous and solid phases, the initial dye concentration provides a significant driving force to overcome any resistance encountered [63]. The removal rates of Y2G, Indigo dyes and the biosorption capacity of *HSP* at different initial dye concentrations varied from 50 mg/L to 300 mg/L and are shown in Fig. 7 It can be clearly seen that the biosorption at different concentrations is rapid in the initial stages and then slows down with time. When the initial Y2G and Indigo dye concentrations increased from 50 to 300 mg/L, the actual amount of dye adsorbed per unit mass of *HSP* increased from 7.87 to 39.76 mg/g and from 14.73 to 85.97 mg/g, respectively. However, maximum dye removal was observed at 150 mg/L (84.87%) and 100 mg/L (88.41%) for Y2G and Indigo dyes. After achieving the maximum point in all the experiments, a leveling off would be observed for further increases in dye concentration – or even a decrease – indicating saturation of all binding sites [32,58,64]. At lower initial dye concentrations, the sorption sites were available for dye adsorption. When the initial dye concentration increased, the available sites might be occupied and ultimately, the dye removal would depend on the initial dye concentration [65].

3.3.4. Effect of agitation speed

Agitation is a significant parameter in sorption phenomena, and it has a serious effect on the distribution of

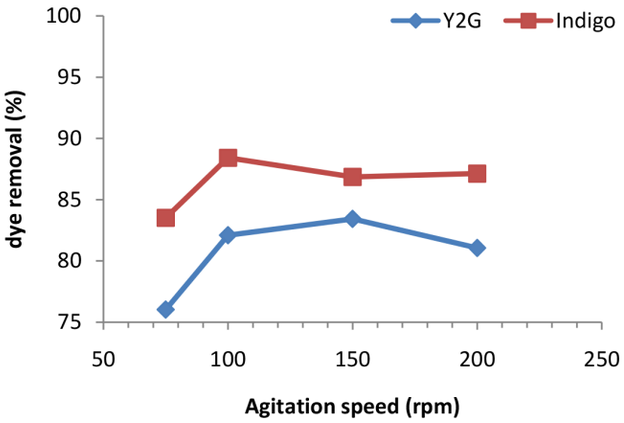

Fig. 8. The effect of agitation speed on the equilibrium biosorption of *S. pacifica*. Experimental conditions: C_o: 150 mg/L, biomass: 5 g/L, temperature: 25°C, pH 2 and time 120 min for Y2G; C_o: 100 mg/L, biomass: 3 g/L, temperature: 25°C, pH2 and time 120 min for Indigo.

the solute in the bulk solution and on the external boundary film formation [65]. When the agitation speed increases, there is increased turbulence, and the thickness of the liquid boundary layer will be decreased as a result of a higher diffusion rate of dye molecules from bulk liquid to the liquid boundary layer surrounding the particles [62].

In the experiments conducted, agitation speeds from 75 to 200 rpm were tested for 120 min (Fig. 8). As seen from Fig. 8, an agitation speed of 150 rpm was optimum for Y2G and 100 rpm was appropriate for the Indigo dye study. Maximum Y2G removal was observed at 83.43% for Y2G at 150 rpm, and 88.42% for Indigo dye at 100 rpm. When the agitation speed was increased to 200 rpm, adsorption capacity decreased due to an increasing desorption tendency. This desorption tendency may be attributed to the high mixing speed, which means more energy input and a higher shear force to break the bonds between the dyes and the adsorbent [65]. An agitation rate of 100–150 rpm is adequate to ensure that all the surface binding sites are made readily available for dye uptake.

3.3.5. Effect of temperature

To investigate the effect of temperature on biosorption of Y2G and Indigo dyes, experiments were carried out at four different temperatures: 20 ± 1, 25 ± 1, 35 ± 1 and 45 ± 1°C at constant Y2G and Indigo concentrations of 150 mg/L and 100 mg/L, and biosorbent doses of 5 g/L and 3 g/L, respectively, at a pH value of 2. It can be clearly seen that the uptake of Y2G and Indigo dyes by the *HSP* decreased with the increase in temperature, which proves the exothermic nature of the biosorption process (Fig. 9) [3,11].

The thermodynamic parameters, including standard enthalpy change (ΔH), entropy change (ΔS) and free energy change (ΔG^o), were calculated to evaluate the feasibility of the biosorption process using the equations given below: [66,67]

$$K_c = \frac{C_{ads}}{C_e} \tag{3}$$

$$\Delta G = -RT \ln K_c \tag{4}$$

$$\Delta G = \Delta H - T\Delta S \tag{5}$$

$$\ln K_c = \frac{\Delta S}{R} - \frac{\Delta H}{RT} \tag{6}$$

In Eq. (3), K_c is the equilibrium constant, C_{ads} represents the amount of dye adsorbed onto *HSP* at equilibrium (mg/g) and C_e is the equilibrium concentration of dye molecules (mg/L). In the fourth equation, R is the universal gas constant (J/mol K) and T is the absolute temperature (Kelvin).

ΔH and ΔS were determined from the slope and intercept of the plot between ln K_c versus 1/T (see Fig. 10).

Negative values of ΔG^o indicate a feasible and spontaneous biosorption nature for the biosorption of Y2G and Indigo dyes. So, it confirms the affinity of *HSP* for Y2G and Indigo biosorption [68]. As seen in Table 2, a negative value of ΔH shows the exothermic characteristics of dye biosorption by *HSP*. For Y2G dye, the physical biosorption process is expected to be dominant as the calculated ΔH value exists in the range from 10 to 40 kJ/mol [69]. Negative values of ΔS represent the uniformity of the solute molecules in the adsorption phenomena [70].

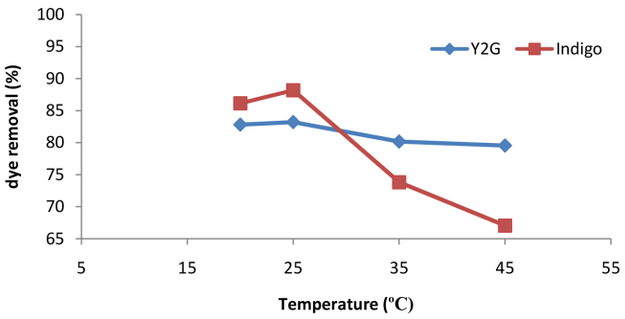

Fig. 9. Effect of temperature on the removal of (a) Y2G (Contact time: 2h, initial concentration of dye 150 mg/L, pH 2.0 and biosorbent dose 5 g/L, 150 rpm), (b) Indigo (Contact time: 2h, initial concentration of dye 100 mg/L, pH 2.0 and biosorbent dose 3 g/L, 100 rpm).

3.4. Evaluation of biosorption process with different isotherm models

The equilibrium isotherm models are significant techniques for explaining the biosorption mechanism [72]. The main aim of the biosorption isotherms are to relate the adsorbate concentration in the bulk to the adsorbed amount at the interface [72]. Several isotherm models are available and three of them: the Langmuir, Freundlich and Temkin isotherm models are the most widely used to describe the biosorption isotherm. Thus, nonlinear Langmuir, Freundlich and Temkin isotherms were selected in this study to examine the amount of Y2G and Indigo dyes adsorbed onto the *HSP* as a function of dye concentration at constant temperature [46].

3.4.1. Langmuir isotherm

In the Langmuir isotherm, adsorption efficiency increases linearly according to the initial adsorbate concentration [73]. The surface is covered with a monolayer at the maximum saturation point, and the adsorbate concentration that is adsorbed to the surface remains constant. Also, adsorption energy is uniform in this isotherm. The adsorption rate is directly proportional to the adsorbate concen-

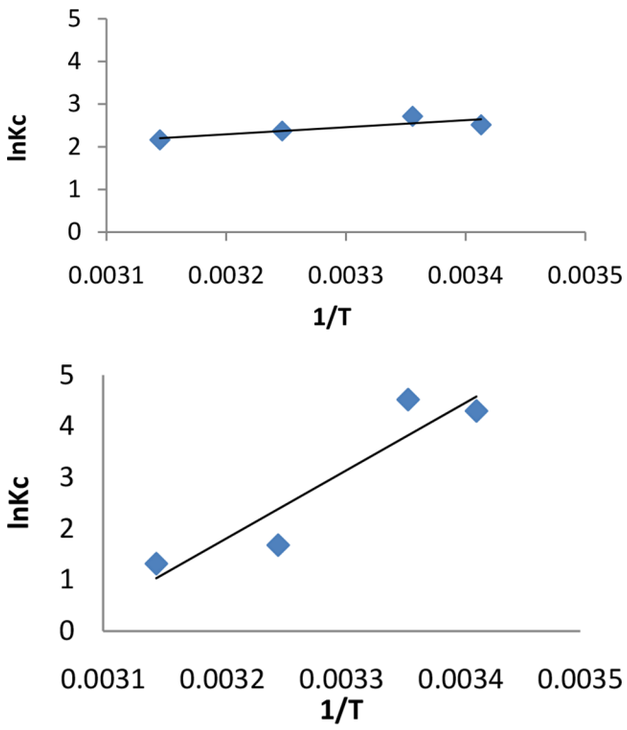

Fig. 10. Van't Hoff plot for the biosorption of Y2G and Indigo dyes by HSP. (a)Y2G (Contact time: 2 h, initial concentration of dye 150 mg/L, pH 2.0 and biosorbent dose 5 g/L, 100 rpm), (b) Indigo (Contact time: 2h, initial concentration of dye 100 mg/L, pH 2.0 and biosorbent dose 3 g/L, 150 rpm).

tration and the active sites on the surface. The Langmuir model is expressed by Eq. (7):

$$q_e = \frac{q_m K_L C_e}{\left(1 + K_L C_e\right)} \tag{7}$$

where q_m (mg/g) is the monolayer adsorption capacity and K_L the empirical equilibrium constant. K_L and q_m have been calculated from the slope and intercept of the Langmuir plot, respectively (Fig. 11). The Langmuir equation can be described by the following linearized form:

$$\frac{C_e}{q_e} = \frac{1}{K_L q_m} + \frac{C_e}{q_m} \tag{8}$$

The linear plot of specific adsorption (C_e/q_e) against equilibrium concentration (C_e) (Fig. 11) gives the q_m and K_L constants. The basic characteristic of the Langmuir isotherm can be expressed by considering a dimensionless separation factor (R_L). The effect of the isotherm shape on whether the biosorption process is suitable or unsuitable can be expressed by parameter R_L. This parameter is expressed by the following equation:

$$R_L = \frac{1}{\left(1 + K_L C_o\right)} \tag{9}$$

where C_o is the maximum initial concentration of adsorbate (mg/L), and K_L (L/mg) is the Langmuir constant. The separation factor R_L can be expressed as the shape of the isotherm as either, unfavorable ($R_L > 1$), linear ($R_L = 1$), favorable ($0 < R_L < 1$), or irreversible ($R_L = 0$). In this study of the biosorption of Y2G and Indigo dyes onto *HSP*, the R_L values were found to be 0.837 and 0.016, respectively (Table 3).

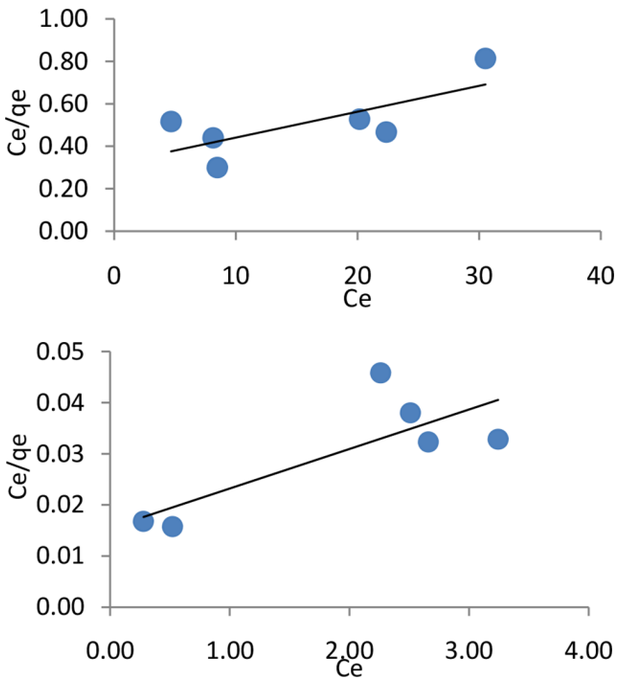

Fig. 11. Langmuir isotherm plots for (a) Y2G and (b) Indigo dyes biosorption onto HSP at 25°C

For favorable isotherms, the R_L values are between 0 and 1. Hence, the biosorptions are favorable.

3.4.2. Freundlich isotherm

The Freundlich isotherm is an empirical equation employed to indicate heterogeneous systems [11]. Freundlich isotherms describe the surface heterogeneity, distribution of the active sites on the surface and their energies. The Freundlich equation is expressed as follows:

$$q_e = K_F + C_e^{\left(\frac{1}{n}\right)} \tag{10}$$

where K_F (mg/g (L/mg)$^{1/n}$) is the biosorption capacity of the sorbent, and n represents the biosorption favorability. The purpose of a Freundlich isotherm is that the detectable constants are integrated into these isotherms [68]. The degree of exponent, $1/n$, describes the favorability of the biosorption process. When $n > 1$, it shows that adsorption is favorable [3]. The degree of exponent, $1/n$, can be expressed as the shape of the isotherm either as: unfavorable ($1/n > 1$), linear ($1/n = 1$), favorable ($0 < 1/n < 1$), or irreversible ($1/n = 0$). In this study, $1/n$ has been calculated to be 0.757 for Y2G and 0.614 for Indigo dyes conforming to the suitability of the biosorption processes performed.

To determine constants K_F and n, the linear form of the equation may be used to produce a graph of $\ln(q_e)$ against $\ln(C_e)$ (Fig. 12).

$$\ln q_e = \ln K_F + \ln C_e \tag{11}$$

Values of K_F and n are calculated from the intercept and slope of the plot (Fig. 12).

3.4.3. Temkin isotherm

The Temkin model assumes that sorbate–adsorbate interactions cause a decrease in heat of adsorption of the molecules in the layer, and bonding energies exhibit uni-

Table 3
Thermodynamic parameters for dye adsorption by using *HSP*

Temperature (K)	ΔG_{Y2G} (kJ/mol)	ΔH^a_{Y2G} (kJ/mol)	ΔS^a_{Y2G} (J/mol K)
293	–6.12		
298	–6.72	–13.42	–23.95
308	–6.07		
318	–5.72		
Temperature (K)	ΔG_{Indigo} (kJ/mol)	ΔH^a_{Indigo} (kJ/mol)	ΔS^a_{Indigo} (J/mol K)
293	–10.47		
298	–11.20	–113.66	–349.63
308	–4.30		
318	–3.48		

[a]Measured between 293 and 333 K.

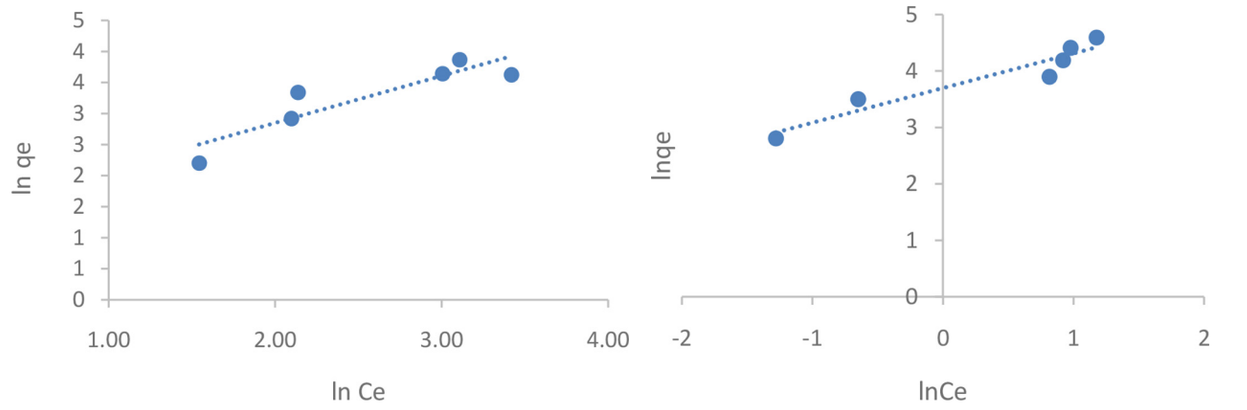

Fig. 12. Freundlich isotherm plots for (a) Y2G and (b) Indigo dyes biosorption onto HSP.

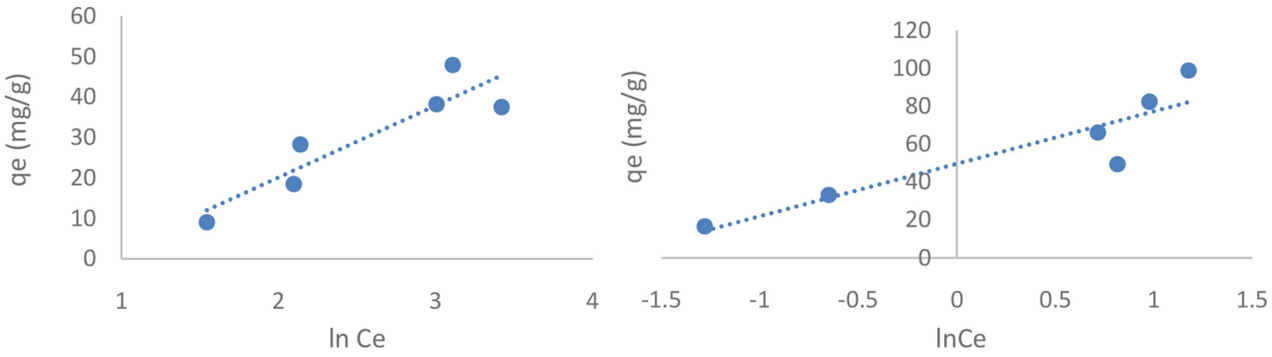

Fig. 13. Temkin isotherm plots for (a) Y2G and (b) Indigo dyes biosorption onto HSP.

Table 4
Isotherm parameters determined for biosorption of dye by using *HSP*

(Y2G)		Langmuir			Freundlich			Temkin	
q_m	K_L	R_L	r^2	K_F	1/*n*	r^2	*A*	*B*	r^2
81.967	0.038	0.208	0.532	21.642	0.76	0.807	0.421	17.76	0.824
(Indigo)		Langmuir			Freundlich			Temkin	
q_m	K_L	R_L	r^2	K_F	1/*n*	r^2	*A*	*B*	r^2
129.87	0,497	0.020	0.627	40.410	0.614	0.913	6.003	27.66	0.821

form distribution in the adsorption process [74]. The Temkin isotherm can be described with the following formula:

$$q_e = \left(\frac{RT}{b}\right)\ln\left(AC_e\right) \tag{12}$$

and can be linearized as:

$$q_e = B\ln A + B\ln C_e \tag{13}$$

where $B = RT/b$, b is the Temkin constant related to the heat of sorption (J/mol); A is the Temkin constant (L/g), R is the gas constant (8.314 J/mol K), and T is the absolute temperature (K). So, plotting q_e versus ln C_e enables one to determine the constants A and b as shown in Fig. 13. The constants A and B are listed in Table 4.

All the isotherm constants and r^2 values obtained are summarized in Table 4.

3.5. Biosorption nature

EDS were employed to explicate the biosorption of both dyes onto *Spirulina pacifica* biosorbent particles. Table 5 displays the data from the EDS elemental analysis of biosorbent particles before and after biosorption. It can be observed in Table 5 that the major elements on the surface of the biosorbent particles before biosorption were C, N, O, P and S.

Table 5
EDS elemental analysis of biosorbent particles before and after biosorption

	Elements (%)[a]				
	C	N	O	P	S
SP* before biosorption	53.73 ± 3.91	33.61 ± 2.76	10.67 ± 1.46	1.05 ± 1.64	0.94 ± 1.48
After SP & Y2G biosorption	54.69 ± 3.75	32.54 ± 2.35	12.23 ± 1.58	0.66 ± 1.29	1.88 ± 2.05
After SP & Indigo biosorption	57.19 ± 4.04	28.65 ± 1.15	11.21 ± 1.10	0.60 ± 1.27	2.84 ± 2.35

[a]Mean values ± standard error obtained from EDS analysis N = 5
**Spiriluna pacifica*

After the biosorption process, the percentage of C, O and S were increased, whereas N and P were decreased. This can be explained by the trapping of dye molecules – containing aromatic rings and sulfonic groups – and which indicates strong interaction between the dyes and the biosorbent particles [13,48] supporting the results of the study. Additionally it also indicates that strong interactions can be explained as characteristics of the chemical interactions and that they are responsible for the higher values of biosorption capacity.

4. Conclusions

This study investigated the biosorption of Y2G and Indigo textile dyes from aqueous solutions by *HSP* algae. Biosorption parameter effects – such as pH value, initial dye concentration, biosorbent dose, agitation speed and temperature – on the removal of Y2G and Indigo dyes has been studied under batch mode operation. The results obtained showed that *HSP* was effective in removing kinds of azo and vat dyes like Y2G and Indigo from aqueous solutions. The optimum conditions were determined to be:

- a pH value of 2, an initial dye concentration of 150 mg/L, a *HSP* dosage of 5 g/L (1g), an agitation speed of 150 rpm and a temperature of 25°C for Y2G dye and,
- a pH value of 2, an initial dye concentration of 100 mg/L, a HSP dosage of 3 g/L (0.6 g), an agitation speed of 100 rpm and a temperature of 25°C for Indigo dye.

The thermodynamic parameters indicated that the processes were spontaneous and exothermic.

The results obtained were modeled using three isotherm models: Langmuir, Freundlich and Temkin. Equilibrium isotherms were successfully described by the Temkin equation for Y2G dye, giving a maximum biosorption of 47.94 mg/g at 2°C (R^2 = 0.824), while the Freundlich equation successfully described the Indigo dye biosorption as 98.7 mg/g at 25°C (R^2 = 0.913).

The FTIR results indicated the main functional groups of *HSP* for biosorption of Y2G and Indigo dye would be amine, hydroxyl, carboxyl, or a combination of those.

Moreover, it is the first study where this commercial, natural nutrient has been used to remove a kind of azo (Y2G) and vat dye (Indigo) from an aqueous solution.

Additionally, *HSP* requires no pretreatment, is ecologically friendly and is a low-cost biosorbent that has a considerable amount of biosorption capacity. This adsorbent is thought to be a promising alternative for the removal of other kinds of dyes, or other organic–inorganic pollutants such as pesticides, endocrine disrupters and heavy metals, from wastewaters.

Acknowledgment

This study was funded by the University of Abant Izzet Baysal Scientific Research Fund under Project No. 2013.09.04.677.

Symbols

A	—	Temkin constant for adsorbate-adsorbate interactions
B	—	Constant related with adsorption heat
b	—	Temkin constant related to heat of sorption
C_e	—	Equilibrium concentration of dye
C_0	—	Initial dye concentration (mg/L)
K_F	—	Freundlich biosorption constant (mg/g)
K_L	—	Langmuir empirical equilibrium constant
q_e	—	Amount of dye per gram of biosorbent at equilibrium (mg/g)
q_m	—	Langmuir biosorption constant (mg/g)
$1/n$	—	Adsorption intensity
R	—	Universal gas constant
R_L	—	Dimensionless separation factor
$R34w^2$	—	Correlation coefficients
W	—	Amount of biosorbent (g)
t	—	Time (min)
T	—	Absolute temperature (K)
V	—	Initial volume of dye solution (L)
$\Delta G°$	—	Standard free energy change (kJ/mol)
ΔH	—	Enthalpy change (kJ/mol)
ΔS	—	Entropy change (kJ/mol)

References

[1] H. Khelifi, Y. Touhami, H. Bouallagui, M. Hamdi, Biosorption of indigo from aqueous solution by dead fungal biomass *Aspergillus alliaceus*, Desal. Wat. Treat., 53(4) (2015) 976–984.
[2] G.B. Oguntimein, Biosorption of dye from textile wastewater effluent onto alkali treated dried sunflower seed hull and design of a batch adsorber, J. Environ. Chem. Eng., 3 (2015) 2647–2661.

[3] İ. Özbay, U. Özdemir, B. Özbay, S. Veli, Kinetic, thermodynamic, and equilibrium studies for adsorption of azo reactive dye onto a novel waste adsorbent: charcoal ash, Desal. Water Treat., 51(31–33) (2013) 6091–6100.
[4] V.K. Gupta, Suhas, Application of low-cost adsorbents for dye removal-a review, J. Environ. Manage., 90(8) (2009) 2313–2342.
[5] A. Mittal, J. Mittal, A. Malviya, V.K. Gupta, Adsorptive removal of hazardous anionic dye "Congo red" from wastewater using waste materials and recovery by desorption. J. Colloid Interface Sci., 340(1) (2009) 16–26.
[6] S. Chowdhury, P. Saha, Adsorption kinetic modeling of safranin onto rice husk biomatrix using pseudo-first- and pseudo-second-order kinetic models: Comparison of linear and non-linear methods, Clean-Soil Air Water, 39(3) (2011) 274–282.
[7] H. Zollinger, Color chemistry: Syntheses, Properties and Applications of Organic Dyes and Pigments. VCH: New York, 1991.
[8] N.F. Cardoso, E.C. Lima, B. Royer, M.V. Bach, G.L. Dotto, L.A.A. Pinto, T. Calvate, Comparison of *Spirulina platensis* microalgae and commercial activated carbon as adsorbents for the removal of Reactive Red 120 dye from aqueous effluents, J. Hazard. Mater., 241–242 (2012) 146–153.
[9] N.F. Cardoso, R.B. Pinto, E.C. Lima, T. Calvete, C.V. Amavisca, B. Royer, M.L. Cunha, T.H.M. Fernandes, I.S. Pinto, Removal of remazol black B textile dye from aqueous solution by adsorption, Desalination, 269 (2011) 92–103.
[10] A.R. Khataee, F. Vafaei, M. Jannatkhah, Biosorption of three textile dyes from contaminated water by filamentous green algal Spirogyra sp.: Kinetic, isotherm and thermodynamic studies, Int. Biodeterior. Biodegradation., 83 (2013) 33–40.
[11] M.T. Sulak, H.C. Yatmaz, Removal of textile dyes from aqueous solutions with eco-friendly biosorbent, Desal. Water Treat., 37 (2012) 169–177.
[12] K. Hunger Industrial Dyes: Chemistry, Properties, Applications. Wiley-VCH Verlag GmbH & Co. KGaA, Weinheim, FRG: Germany, 2003.
[13] Z. Aksu, Application of biosorption for the removal of organic pollutants: a review. Proc. Biochem., 40(3–4) (2005) 997–1026.
[14] T.V. Zee, I. Bisschops, V. Blanchard, R. Bouwman, G. Lettinga J. Field, The contribution of biotic and abiotic processes during azo dye reduction in anaerobic sludge, Water Res., 37(13) (2003) 3098–3109.
[15] Y.H. Lee, S.G. Pavlostathis, Decolorization and toxicity of reactive anthraquinone textile dyes under methanogenic conditions, Water Res., 38(7) (2004) 1838–1852.
[16] M. Neamtu, L. Siminiceanu, A. Yediler, A. Kettrup, Kinetics of decolorization and mineralization of reactive azo dyes in aqueous solution by the UV/H_2O_2 oxidation, Dyes Pigm., 53 (2002) 93–99.
[17] E. Forgacs, T. Cserhati, G. Oros, Removal of synthetic dyes from wastewaters: A review, Environ. Int., 30 (2004) 953–971.
[18] J.F. Gao, Q. Zhang, K. Su, J.H. Wang, Competitive biosorption of Yellow 2G and Reactive Brilliant Red K-2G onto inactive aerobic granules: Simultaneous determination of two dyes by first-order derivative spectrophotometry and isotherm studies, Bioresour. Technol., 101(15) (2010) 5793–5801.
[19] L.W. Lackey, R.O. Mines, P.T. McCreanor, Ozonation of acid yellow 17 dye in a semi-batch bubble column, J. Hazard. Mater., 138(2) (2006) 357–362.
[20] G. Dogdu, A. Yalcuk, Evaluation of the treatment performance of lab-scaled vertical flow constructed wetlands in removal of organic compounds, color and nutrients in azo dye-containing wastewater, Int. J. Phytoremediat., 18(2) (2015) 171–183.
[21] A. Vuorema, Reduction and Analysis Methods of Indigo, Turun Tliopistan Julkaisuja, Annalaes Universitatis Turkuensis, Turku-Finland, (2008) 1–72. www.doria.fi/bitstream/handle/10024/42825/AI388%20Vuorema.pdf (accessed: April 2015).
[22] M. Irimia-Vladu, E.D. Głowacki, P.A. Troshin, G. Schwabegger, L. Leonat, D.K. Susarova, O. Krystal, M. Ullah, Y. Kanbur, M.A. Bodea, V.F. Razumov, H. Sitter, S. Bauer, N.S. Sariciftci, Indigo - A natural pigment for high performance ambipolar organic field effect transistors and circuits, Adv. Mater., 24(3) (2012) 375–380.
[23] M. Vedrenne, R. Vasquez-Medrano, D. Prato-Garcia, B.A. Frontana-Uribe, M. Hernandez-Esparza, J.M. de Andre´s, A ferrous oxalate mediated photo-Fenton system: Toward an increased biodegradability of indigo dyed wastewaters, J. Hazard. Mater., 243 (2012) 292–301.
[24] K.H. Ferber, Toxicology of İndigo: A review, J. Environ. Pathol. Toxicol. Oncol., 7(4) (1987) 73–83.
[25] A. Pirkarami, M.E. Olya, Removal of dye from industrial wastewater with an emphasis on improving economic efficiency and degradation mechanism, J. Saudi Chem. Soc., (2014) 1–8.
[26] M.A. Rauf, S.S. Ashraf, Survey of recent trends in biochemically assisted degradation of dyes, Chem. Eng. J., 209 (2012) 520–530.
[27] S.E. Mbuligwe, Comparative treatment of dye-rich wastewater in engineered wetland systems (EWSs) vegetated with different plants, Water Res., 39(2–3) (2005) 271–280.
[28] N.K. Amin, Removal of direct blue-106 dye from aqueous solution using new activated carbons developed from pomegranate peel: Adsorption equilibrium and kinetics, J. Hazard. Mater., 165(1–3) (2009) 52–62.
[29] E.M. Ayan, P. Secim, S. Karakaya, J. Yanik, Oreganum stalks as a new biosorbent to remove textile dyes from aqueous solutions, CLEAN-Soil Air Water, 40(8) (2012) 856–863.
[30] X.S. Wang, J.P. Chen, Removal of the azo dye Congo red from aqueous solutions by the marine alga Porphyra yezoensis Ueda, CLEAN-Soil Air Water, 37(10) (2009) 793–798.
[31] M.E. Russo, F. Di Natale, V. Prigione, V. Tigini, A. Marzocchella G.C. Varese, Adsorption of acid dyes of fungal biomass: Equilibrium and kinetics characterization, Chem. Eng. J., 162(2) (2010) 537–545.
[32] R. Rakhshaee, Rule of Fe° nano-particles and biopolymer structures in kinds of the connected pairs to remove Acid Yellow 17 from aqueous solution: Simultaneous removal of dye in two paths and by four mechanisms, J. Hazard. Mater., 197 (2011) 144–152.
[33] J. Gao, Q. Zhang, K. Su, R. Chen, Y. Peng, Biosorption of Acid Yellow 17 from aqueous solution by non-living aerobic granular sludge, J. Hazard. Mater., 174 (2010) 215–225.
[34] E. Acuner, F.B. Dilek, Treatment of tectilon yellow 2G by Chlorella vulgaris, Process Biochem., 39 (2004) 623–631.
[35] V.O. Njoku, K.Y. Foo, M. Asif, B.H. Hameed, Preparation of activated carbons from rambutan (Nephelium lappaceum) peel by microwave-induced KOH activation for acid yellow 17 dye adsorption, Chem. Eng. J., 250 (2014) 198–204.
[36] R. Sivaraj, C. Namasivayam, K. Kadirvelu, Orange peel as an adsorbent in the removal of Acid violet 17 (acid dye) from aqueous solutions, Waste Manage., 21 (2001) 105–110.
[37] M. Ozacar, I.A. Sengil, Adsorption of acid dyes from aqueous solutions by calcined alunite and granular activated carbon, Adsorption, 8 (2002) 301–308.
[38] S. Aber, M. Sheydaei, Removal of COD from ındustrial effluent containing ındigo dye using adsorption method by activated carbon cloth: optimization, kinetic, and ısotherm studies, CLEAN-Soil Air Water, 40(1) (2012) 87–94.
[39] M. Otero, F. Rozada, L.F. Calvo, A.I. Garca, A. Moran, Elimination of organic water pollutants using adsorbents obtained from sewage sludge, Dyes Pigm., 57 (2003) 55–65.
[40] G.L. Dotto, L.A.A. Pinto, Analysis of mass transfer kinetics in the biosorption of synthetic dyes onto *Spirulina platensis* nanoparticles, Biochem Eng J., 68 (2012) 85–90.
[41] F. Deniz, R.A. Kepekci, Dye biosorption onto pistachio by-product: A green environmental engineering approach, J. Mol. Liq., 219 (2016)194–200.
[42] ULR1, BIOAGE, http://bioage.com/ingredients.html (accessed: May 2016).
[43] ULR2, Spirulina-Natures Miracle Plant Food, www.earthworks.com/spirulina/index.html (Acessed: Februrary 2016).
[44] V.K. Gupta, A. Mittal, V. Gajbe, Adsorption and desorption studies of a water soluble dye, Quinoline Yellow, using waste materials, J. Colloid Interface Sci., 284 (2005) 89–98.
[45] V.K. Gupta, I. Ali, Suhas, D. Mohan, Equilibrium uptake and sorption dynamics for the removal of a basic dye (basic red) using low-cost adsorbents, J. Colloid Interface Sci., 265 (2003) 257–264.

[46] A. Çelekli, H. Bozkurt, Bio-sorption of cadmium and nickel ions using *Spirulina platensis*: Kinetic and equilibrium studies, Desalination, 275 (2011) 141–147.
[47] N. Barka, M. Abdennouri, M. El Makhfouk, Removal of Methylene Blue and Eriochrome Black T from aqueous solutions by biosorption on Scolymus hispanicus L.: Kinetics, equilibrium and thermodynamics, J. Taiwan Inst. Chem. E., 42 (2011) 320–326.
[48] G.L. Dotto, T.R.S. Cadaval, L.A.A. Pinto, Use of Spirulina platensis micro and nanoparticles for the removal synthetic dyes from aqeous solutions by biosorption, Proc. Biochem., 47 (2012) 1335–1343.
[49] T. Calvete, E.C. Lima, N.F. Cardoso, S.L.P. Dias, F.A. Pavan, Application of carbon adsorbents prepared from the Brazilian-pine fruit shell for removal of Procion Red MX 3B from aqueous solution – kinetic, equilibrium, and thermodynamic studies, Chem. Eng. J., 155 (2009) 627–636.
[50] A. Çelekli, M. Yavuzatmaca, Predictive modeling of biomass production by Spirulina platensis as function of nitrate and NaCl concentrations, Bioresour. Technol., 100(5) (2009) 1847–1851.
[51] A. Çelekli, M. Yavuzatmaca, H. Bozkurt, An eco-friendly process: predictive modeling of copper adsorption from aqueous solution on Spirulina platensis, J. Hazard. Mater. 173(1–3) (2010)123–129.
[52] E. Daneshvar, M. Kousha, M. Jokar, N. Koutahzadeh, E. Guibal, Acidic dye biosorption onto marine Brown microalgae: Isotherms, kinetic and thermodynamic studies, Chem. Eng., J. 204–206 (2012) 225–234.
[53] A. Çelekli, H. Bozkurt, Biosorption of cadmium and nickel ions using Spirulina platensis – kinetic and equilibrium studies, Desalination, 275 (2011) 141–147.
[54] R. Elmoubarkia, F.Z. Mahjoubia, H. Tounsadia, J. Moustadrafa, M. Abdennouria, A. Zouhrib, A. El Albanic, N. Barkaa, Adsorption of textile dyes on raw and decanted Moroccan clays: Kinetics, equilibrium and thermodynamics, Water Res. Ind., 9 (2015) 16–29.
[55] K.Y. Foo, B.H. Hameed, Adsorption characteristics of industrial solid waste derived activated carbon prepared by microwave heating for methylene blue, Fuel Process Technol., 99 (2012) 103–109.
[56] M, Benadjemia, L. Milliere, L. Reinert, N. Benderdouche, L. Duclaux, Preparation, characterization and methylene Blue adsorption of phosphoric acid activated carbons from globe artichoke leaves, Fuel Process. Technol., 92 (2011) 1203–1212.
[57] Y. Xi, Y. Shen, F. Yanf, G. Yang, C. Liu, Z. Zhang, D. Zhu, Removal of azo dye from aqueous solution by a new biosorbent prepared with Aspergillus *nidulans* cultured in tobacco wastewater, J. Taiwan Inst. Chem. E., 44(5) (2013) 815–820.
[58] M.U. Din, H.N. Bhatti, M. Yasir, A. Ashraf, Direct dye biosorption by immobilized barley husk, Desal. Water Treat., 57 (2016) 9263–9271.
[59] L.S. Krishna, A. Yuzir, G. Yuvaraja, V.A. Kumar, Removal of Acid blue 25 from aqueous solutions by using Bengal gram fruit shell (BGFS) biomass, Int. J. Phytoremediation., (*In press.)* doi:10.1080/15226514.2016.1256372.
[60] S. Dawood, T.K. Sen, Removal of anionic dye Congo red from aqueous solution by raw pine and acid-treated pine cone powder as adsorbent: Equilibrium, thermodynamic, kinetics, mechanism and process design, Water Res., 46 (2012) 1933–1946.
[61] K.G. Bhattacharyya, A. Sharma, Adsorption of Pb(II) from aqueous solution by Azadirachta indica (Neem) leaf powder, J. Hazard. Mater., 113(1–3) (2004) 97–109.
[62] B.K. Suyamboo, R.S. Perumal, Equilibrium, thermodynamic and kinetic studies on adsorption of a basic dye by Citrullus Lanatus Rind, Iranica, J. Energy Environ., 3(1) (2012) 23–34.
[63] N. Caner, I. Kiran, S. Ilhan, C.F. Iscen, Isotherm and kinetic studies of Burazol Blue ED dye biosorption by dried anaerobic sludge, J. Hazard. Mater., 165 (2009) 279–284.
[64] B.H. Hameed, D.K. Mahmoud, A.L. Ahmad, Equilibrium modeling and kinetic studies on the adsorption of basic dye by a low-cost adsorbent: Coconut (Cocos nucifera) bunch waste, J. Hazard. Mater., 158 (2008) 65–72.
[65] M.M. Abd El-Latif, A.M. Ibrahim, M.F. El-Kady, Adsorption Equilibrium, kinetics and thermodynamics of methylene blue from aqueous solutions using bipolymer oak sawdust composite, J. Am. Sci., 6(6) (2010) 267–283.
[66] N. Gupta, A.K. Kushwaha, M.C. Chattopadhyaya, Adsorption studies of cationic dyes onto Ashoka (*Saraca asoca*) leaf powder, J. Taiwan Inst. Chem. E., 43 (2012) 604–613.
[67] T. Robinson, B. Chandran, P. Nigam, Removal of dyes from a synthetic textile dye effluent by biosorption on apple pomace and wheat straw, Water Res., 36(11) (2002) 2824–2830.
[68] M. Jerold, V. Sivasubramanian, Biosorptive removal of malachite green from aqueous solution using chemically modified brown marine alga Sargassum swartzii, Water Sci. Technol., (*In press.)* doi: 10.2166/wst.2016.513.
[69] Z.M. Jiang, A.M. Li, J. Cai, C. Wang, Q. Zhang, Adsorption of phenolic compounds from aqeous solutions by aminated hypercrosslinked polymers, J. Environ. Sci., 19 (2007) 135–140.
[70] U. Özdemir, B. Özbay, S. Veli, S. Zor, Modeling adsorption of sodium dodecyl benzene sulfonate (SDBS) onto polyaniline (PANI) by using multi linear regression and artificial neural networks, Chem. Eng. J, 178 (2011) 183–190.
[71] T. Akar, M. Divrikoğlu, Biosorption applications of modified fungal biomass for decolorization of Reactive Red 2 contaminated solutions: Batch and dynamic flow mode studies, Biores. Technol., 101(19) (2010) 7271–7277.
[72] J. Eastoe, J.S. Dalton, Dynamic surface tension and adsorption mechanisms of surfactants at the air–water interface, Desalination, 85(2–3) (2000) 103–144.
[73] I. Langmuir, The constitution and fundamental properties of solids and liquids Part I. Solids, J. Am. Chem. Soc., 38 (11) (1916) 2221–2295.
[74] M.I. Tempkin, V. Pyzhev, Kinetics of ammonia synthesis on promoted iron catalyst, Acta Phys. Chim. USSR, 12 (1940) 327–356.

Supplementary material

Specifications and General Composition of Biosorbent

General Description	Spirulina *pacifica*™ is a dried and non-viable product of the common blue-green algae, Arthrospira *platensis* (formerly referred to as Spirulina *platensis*). This species is classified as follows:
	Order: Oscillatoriales
	Family: Cyanobacteria
	Genus: Arthrospira
	Species: platensis
Physical Properties	Spirulina *pacifica*™ is a free-flowing green to bluish-green powder. It has a mild seaweed odor and is not soluble; it forms a suspension.
	The Particle size is <125 microns
	Bulk Density is >0.48 (g/ml).
Typical Composition	Protein: >52%
	Moisture: <7.0%
	Minerals: <14%
	Total carotenoids: >5000 mg/kg
	Beta-carotene: >2250 mg/kg
	Zeaxanthin: 3000 mg/kg
	C-phycocyanin: 8.0%
	Phycocyanin (crude): >17.3%
	Vitamin B12: 3000 mcg/kg
	Vitamin K: 20 mg/kg